

## On the Formulation of Finite-Element Prediction Models

R. T. WILLIAMS

*Department of Meteorology, Naval Postgraduate School, Monterey, CA 93940*

(Manuscript received 19 March 1980, in final form 7 July 1980)

### ABSTRACT

Three numerical schemes for the vorticity-divergence form of the shallow-water equations are analyzed using the Fourier transform technique developed by Schoenstadt (1980). These schemes are compared with two finite-element schemes for the primitive form of the equations which were examined by Schoenstadt. The best finite-element schemes use either staggered elements in the primitive form of the equations, or unstaggered elements in the vorticity-divergence form.

### 1. Introduction

The finite-element method (FEM), which was developed in engineering statics, has recently been used in various atmospheric prediction models (Cullen, 1974; Hinsman, 1975; Staniforth and Mitchell, 1977, 1978). The FEM is a special case of the Galerkin procedure in which the dependent variables are approximated by a finite sum of spatially varying basis functions with time-dependent coefficients. The FEM basis functions are low order polynomials which are zero except in a localized region. The Galerkin procedure produces a set of coupled ordinary differential equations for the coefficients which are solved by introducing finite differences in time (see, e.g., Pinder and Gray, 1977).

FEM models are potentially more accurate than finite difference models, but they normally require more computational effort per degree of freedom. Kelley and Williams (1976) found considerable small-scale noise in an FEM formulation of the shallow-water equations in a channel. In that study the same basis functions were used for all of the dependent variables. Winninghoff (1968), Arakawa and Lamb (1977) and Schoenstadt (1980) have demonstrated the advantages of spatial staggering of dependent variables in finite difference models. Schoenstadt (1980) also examined FEM schemes in which the basis functions for different dependent variables were staggered and he found much better behavior than when they were unstaggered. Also, Staniforth and Mitchell (1977, 1978) have obtained excellent results with a vorticity-divergence FEM formulation. Cullen and Hall (1979) have found the vorticity-divergence formulation to be superior in a comparison between various FEM global models.

This paper will examine the response of several numerical schemes to small-scale initial conditions

or small-scale forcing. An efficient finite-element model must handle small-scale motions smoothly; otherwise extra degrees of freedom will be required because the smallest scales must be smoothed to keep them from spuriously affecting larger scale fields. The various schemes will be compared by treating the geostrophic adjustment process with the Fourier transform procedure that was developed by Schoenstadt (1980).

### 2. Basic equations

The linearized shallow-water equations with no mean flow can be written as

$$\frac{\partial u}{\partial t} - fv + g \frac{\partial h}{\partial x} = 0, \quad (2.1)$$

$$\frac{\partial v}{\partial t} + fu = 0, \quad (2.2)$$

$$\frac{\partial h}{\partial t} + H \frac{\partial u}{\partial x} = 0, \quad (2.3)$$

where  $u$  and  $v$  are the perturbation velocities in the  $x$  and  $y$  directions, respectively, and  $H$  and  $h$  the mean and perturbed heights of the free surface. Also  $g$  represents gravity and  $f$  is the Coriolis parameter. Note that all quantities are independent of  $y$ .

The vorticity and divergence equations, which are particularly simple in one dimension, are obtained by differentiating (2.1) and (2.2) with respect to  $x$  which yields

$$\frac{\partial D}{\partial t} - f\zeta + g \frac{\partial^2 h}{\partial x^2} = 0, \quad (2.4)$$

$$\frac{\partial \zeta}{\partial t} + fD = 0, \quad (2.5)$$

$$\frac{\partial h}{\partial t} + HD = 0, \tag{2.6}$$

where  $D = \partial u/\partial x$  is the divergence and  $\zeta = \partial v/\partial x$  is the vorticity.

Schoenstadt (1977) solved the continuous equations (2.1)–(2.3) with the spatial Fourier transform. We will apply the same procedure to the vorticity-divergence equations (2.4)–(2.6). If we denote Fourier transforms by a tilde, such as

$$\tilde{D}(k,t) = \int_{-\infty}^{\infty} D(x,t)e^{-ikx}dx, \tag{2.7}$$

then the transformed vorticity-divergence set (2.4)–(2.6) may be written as

$$\frac{d\tilde{D}}{dt} - f\tilde{\zeta} - \mu^2 g\tilde{h} = 0, \tag{2.8}$$

$$\frac{d\tilde{\zeta}}{dt} + f\tilde{D} = 0, \tag{2.9}$$

$$\frac{d\tilde{h}}{dt} + H\tilde{D} = 0, \tag{2.10}$$

where  $\mu^2 = k^2$  is introduced for convenience later. The solution to this set is given by

$$\tilde{D}(k,t) = \tilde{D}_0 \cos \nu t + \frac{f\tilde{\zeta}_0}{\nu} \sin \nu t + \frac{\mu^2 g h_0}{\nu} \sin \nu t, \tag{2.11}$$

$$\begin{aligned} \tilde{\zeta}(k,t) = & -\frac{f\tilde{D}_0}{\nu} \sin \nu t + \left( \frac{\mu^2 g H}{\nu^2} + \frac{f^2}{\nu^2} \cos \nu t \right) \tilde{\zeta}_0 \\ & - \frac{\mu^2 f}{\nu^2} (1 - \cos \nu t) g \tilde{h}_0, \end{aligned} \tag{2.12}$$

$$\begin{aligned} \tilde{h}(k,t) = & -\frac{H\tilde{D}_0}{\nu} \sin \nu t - \frac{Hf}{\nu^2} (1 - \cos \nu t) \tilde{\zeta}_0 \\ & + \left( \frac{f^2}{\nu^2} + \frac{\mu^2 g H}{\nu^2} \cos \nu t \right) \tilde{h}_0, \end{aligned} \tag{2.13}$$

where

$$\nu^2 = f^2 + \mu^2 g H. \tag{2.14}$$

The initial conditions are written

$$\tilde{D}_0 = \tilde{D}(k,0) = \int_{-\infty}^{\infty} D(x,0)e^{-ikx}dx, \tag{2.15}$$

with similar definitions for  $\tilde{\zeta}_0$  and  $\tilde{h}_0$ .

### 3. Finite-difference and finite-element solutions

Schoenstadt (1980) carried out a general analysis of the solutions to (2.1)–(2.3) which allowed for spatially centered finite differences or finite elements. We will use the same method to obtain certain finite-difference and finite-element solutions to system (2.4)–(2.6). Following Schoenstadt (1980) the Fourier transformed versions of the various numerical schemes for Eqs. (2.4)–(2.6) can be written in the form

$$\alpha \frac{d\tilde{D}}{dt} - \alpha f \tilde{\zeta} - \sigma^2 g \tilde{h} = 0, \tag{3.1}$$

$$\gamma \frac{d\tilde{\zeta}}{dt} + f \gamma \tilde{D} = 0, \tag{3.2}$$

$$\gamma \frac{d\tilde{h}}{dt} + H \gamma \tilde{D} = 0, \tag{3.3}$$

where  $\alpha(k)$ ,  $\gamma(k)$  and  $\sigma(k)$  are given in Table 1. This set can be put in the same form as (2.8)–(2.10) by dividing  $\alpha$  or  $\gamma$  and setting

$$\mu^2 = \sigma^2/\alpha. \tag{3.4}$$

The frequency equation (2.14) becomes

$$\nu^2 = f^2 + (\sigma^2/\alpha)gH. \tag{3.5}$$

The solutions to set (3.1)–(3.3) are given by (2.11)–(2.13) with the use of (3.4) and (3.5).

Table 1 contains the parameters for a finite-difference and two finite-element versions of the vorticity-divergence set of equations. In scheme 1  $D$ ,  $\zeta$  and  $h$  are carried at the same points, and  $\partial^2 h/\partial x^2$  is approximated with  $[h(x + \Delta x) - 2h(x) + h(x - \Delta x)]/\Delta x^2$ , where  $\Delta x$  is the grid spacing. The equations for scheme 2 are obtained by applying the Galerkin method to the system (2.4)–(2.6) with linear functions (see, e.g., Chap. 6 in Haltiner and Williams, 1980). Scheme 3 which was suggested by Dr. A. Staniforth (private communication) uses a higher order mass matrix in the divergence equation (see also Staniforth and Mitchell, 1977). This matrix has coefficients ( $1/12$ ,  $5/6$ ,  $1/12$ ) as compared with ( $1/6$ ,  $2/3$ ,  $1/6$ ) for the mass matrix used in the other equations and in scheme 2.

The solutions (2.11)–(2.13) differ for the various numerical schemes only through  $1/\nu$  and  $\mu/\nu$  which appear in various coefficients in the solutions. Con-

TABLE 1. Parameters for a finite-difference and two finite-element versions of the vorticity-divergence set of equations.

Scheme	Type differential	$\alpha$ 1	$\gamma$ 1	$\sigma^2$ $k^2$
1	finite difference	1	1	$\sin^2(k\Delta x/2)/(\Delta x/2)^2$
2	FEM	$[2 + \cos(k\Delta x)]/3$	$[2 + \cos(k\Delta x)]/3$	$\sin^2(k\Delta x/2)/(\Delta x/2)^2$
3	FEM	$[5 + \cos(k\Delta x)]/6$	$[2 + \cos(k\Delta x)]/3$	$\sin^2(k\Delta x/2)/(\Delta x/2)^2$

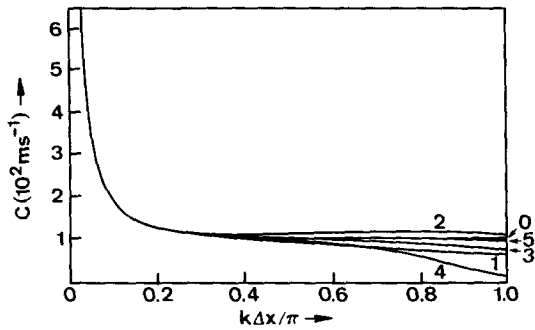


FIG. 1. The phase velocity  $c = v/\mu$  as a function of  $k\Delta x/\pi$  for the various schemes. The analytic solution is labeled with 0. These results use the following values:  $gH = 10^4 \text{ m}^2 \text{ s}^{-2}$ ,  $f = 10^{-4} \text{ s}^{-1}$ ,  $\Delta x = 500 \text{ km}$ .

siderable information about the behavior of the various schemes can be obtained by examining these quantities as functions of  $k\Delta x/\pi$ . We will compare the vorticity-divergence schemes in Table 1 with the following two finite-element schemes for the primitive equations (2.1)–(2.3) which were analyzed by Schoenstadt (1980):

- scheme 4—unstaggered nodal points (also known as FEM A),
- scheme 5—staggered nodal points (also known as FEM B).

Both of these schemes use piecewise linear basis functions, but scheme 5 has velocity nodal points midway between height nodal points (a basis function is a maximum at its nodal point). More information on these schemes is given by Schoenstadt (1980).

Fig. 1 contains the phase speed,  $c = v/k$ , as a function of  $k\Delta x/\pi$  for the various schemes from (3.5) or as obtained from Schoenstadt (1980). The exact solution is labeled with a zero, and the other curves are labeled with the scheme number. The unstaggered FEM formulation (scheme 4) of (2.1)–(2.3) gives the poorest phase speeds for the short wavelengths, whereas the staggered FEM formulation (scheme 5) gives the best. The FEM schemes 2 and 3 based on (2.4)–(2.6) are reasonably good with scheme 3 being superior, except for the smallest scales. The finite-difference formulation (scheme 1) of (2.4)–(2.6) is still much better than the unstaggered FEM version (scheme 4) of (2.1)–(2.3).

Fig. 2 contains the group velocity  $G = dv/dk$  as a function of  $k\Delta x/\pi$  for the same schemes. Scheme 4 is extremely poor for small scales since it propagates energy rapidly in the wrong direction. Scheme 5 is again the best scheme and scheme 3 is better than scheme 2 except for the smallest scales.

Fig. 3 gives the coefficient  $1/\nu$  as a function of  $k\Delta x/\pi$  for the various schemes. This coefficient is especially important since  $1/\nu^2$  relates the final (steady-state) height to the initial height field [see

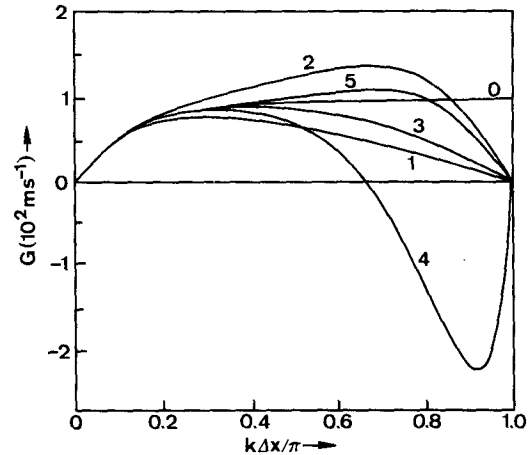


FIG. 2. The group velocity  $G = dv/dk$  for the same conditions as Fig. 1.

(2.13)]. Scheme 4 is very bad for the short wavelengths, and scheme 5 is again the best. All of the vorticity-divergence schemes are good with 3 being the best except for the smallest scales.

Fig. 4 contains the coefficient  $\mu/\nu$  as a function of  $k\Delta x/\pi$  for the various schemes. Scheme 4 is very poor as is the case in the other figures. All of the other schemes are very close to the exact solution.

#### 4. Conclusions

Schoenstadt (1980) showed that the unstaggered finite element formulation of the shallow-water equations (scheme 4) has very poor geostrophic adjustment properties. The short waves propagate energy rapidly in the wrong direction (see Fig. 2) which distorts geostrophic adjustment and leads to rapid

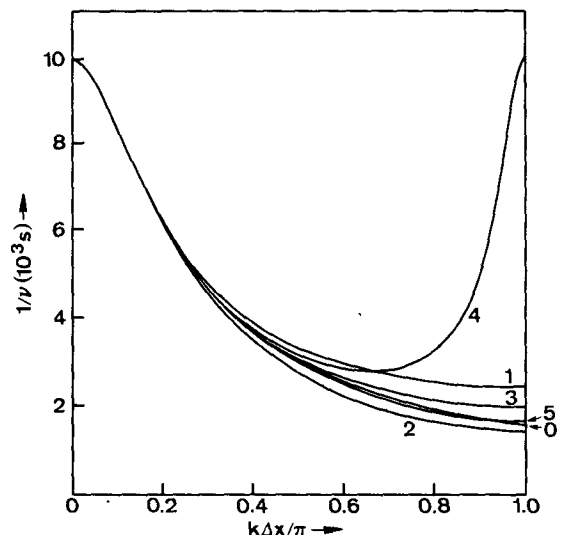


FIG. 3. The coefficient  $1/\nu$  for the same conditions as Fig. 1.

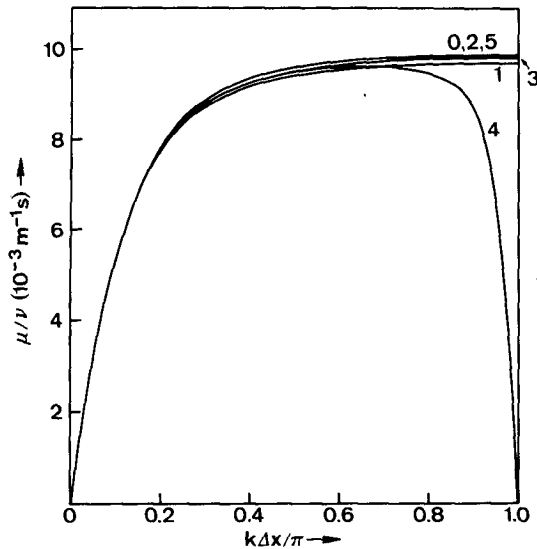


FIG. 4. The coefficient  $\mu/\nu$  for the same conditions as Fig. 1.

spreading of numerical errors. This scheme also produces a very noisy height field after geostrophic adjustment because the coefficient  $1/\nu^2$  is 25 times too large for the shortest wave (see Fig. 3). Schoenstadt (1980) also found that a finite-element formulation with the velocity nodal points midway between height nodal points (scheme 5) is excellent in regard to geostrophic adjustment.

In this paper the Schoenstadt analysis procedure was applied to three schemes that are based on the vorticity-divergence form of the shallow-water equations. All of the schemes have much better geostrophic adjustment properties than scheme 4. The finite difference version (scheme 1) gives the same curves as the staggered primitive equation finite-difference formulation with velocity points between height points (also known as scheme B), that was examined by Schoenstadt (1980). Finite element scheme 3 is slightly better than scheme 2, but neither is quite as good as scheme 5. These results show that the behavior of primitive equation schemes with proper staggering is very similar to the behavior of unstaggered vorticity-divergence schemes. This is because approximations for  $\partial^2 h/\partial x^2$  in (2.4) which involve these adjacent points are consistent with approximations for  $\partial h/\partial x$  and  $\partial u/\partial x$  in (2.1) and (2.3), which involve two adjacent points.

This analysis strongly indicates that finite-element formulations of the shallow-water equations should not use the primitive form of the equations with unstaggered nodal points. If such formulations are used, smoothing will be required to control small scale noise as discussed by Cullen (1976). This will necessitate a smaller grid size because of the lost accuracy in the small scales. It would be better to

use either the staggered scheme 5 or the vorticity-divergence schemes 2 or 3, since these schemes give smooth responses to small-scale initial conditions. This should be especially true in two dimensions even though these schemes require about one-half the time step which can be used with scheme 4. The choice between schemes 2, 3 or 5 should depend on other considerations which are not included in this paper.

*Acknowledgments.* The author wishes to thank Professors G. J. Haltiner, A. L. Schoenstadt and Dr. A. Staniforth for reading the manuscript and for making constructive comments. This research was supported by the Naval Air Systems Command through the Naval Environmental Prediction Research Facility, and the Fleet Numerical Oceanography Center. The numerical computations were performed by the W. R. Church Computer Center. The manuscript was carefully typed by Ms. M. Marks and the figures were drafted by Mr. M. McDermet.

#### REFERENCES

- Arakawa, A., and V. Lamb, 1977: Computational design of the basic dynamical processes of the UCLA General Circulation Model. *Methods of Computational Physics*, Vol. 17, Academic Press, 174–266.
- Cullen, M. J. P., 1974: Integration of the primitive equations on a sphere using the finite element method. *Quart. J. Roy. Meteor. Soc.*, **100**, 555–562.
- , 1976: On the use of artificial smoothing in Galerkin and finite difference solutions of the primitive equations. *Quart. J. Roy. Meteor. Soc.*, **102**, 77–93.
- Cullen, M. J. P., and C. D. Hall, 1979: Forecasting and general circulation results from finite element models. *Quart. J. Roy. Meteor. Soc.*, **105**, 571–592.
- Haltiner, G. J., and R. T. Williams, 1980: *Numerical Prediction and Dynamic Meteorology*. Wiley, 477 pp.
- Hinsman, D. E., 1975: Application of a finite element method to the barotropic primitive equations. M.S. thesis, Naval Postgraduate School, Monterey, CA, 116 pp.
- Kelley, R. G., and R. T. Williams, 1976: A finite element prediction model with variable element sizes. Naval Postgraduate School Report NPS-63Wu76101, 109 pp.
- Pinder, G. F., and W. G. Gray, 1977: *Finite Element Simulation in Surface and Subsurface Hydrology*. Academic Press, 295 pp.
- Schoenstadt, A., 1977: The effect of spatial discretization on the steady-state and transient behavior of a dispersive wave equation. *J. Comput. Phys.*, **23**, 364–379.
- , 1980: A transfer function analysis of numerical schemes used to simulate geostrophic adjustment. *Mon. Wea. Rev.*, **108**, 1248–1259.
- Staniforth, A. N., and H. L. Mitchell, 1977: A semi-implicit finite-element barotropic model. *Mon. Wea. Rev.*, **105**, 154–169.
- , 1978: A variable-resolution finite-element technique for regional forecasting with the primitive equations. *Mon. Wea. Rev.*, **106**, 439–447.
- Winninghoff, F., 1968: On the adjustment toward a geostrophic balance in a simple primitive equation model with application to the problem on initialization and objective analysis. Ph.D. dissertation, UCLA, 161 pp.